Proceedings of the ASME 2021 Conference on Smart Materials, Adaptive Structures and Intelligent Systems
SMASIS 2022
September 12-14, 2022, Dearborn (MI), USA

SMASIS2022-90623

NONLINEAR DYNAMICS OF A TWO MEMBER ANGLE-SHAPED ENERGY HARVESTER

Francesco Danzi*
School of Mechanical Engineering
and Ray W. Herrick Laboratories
Purdue University
West Lafayette, Indiana, 47907
Email: fdanzi@purdue.edu

Amin Joodaky
School of Packaging
Michigan State University
East Lansing, Michigan, 48824
Email: joodakya@msu.edu

Hongcheng Tao
School of Mechanical Engineering
and Ray W. Herrick Laboratories
Purdue University
West Lafayette, Indiana, 47907
Email: taoh@purdue.edu

James M. Gibert
School of Mechanical Engineering
and Ray W. Herrick Laboratories
Purdue University
West Lafayette, Indiana, 47907
Email: jgibert@purdue.edu

ABSTRACT

In this article we propose a theoretical investigation of the nonlinear dynamical response of a class of planar resonators dubbed the V-Shaped resonator. The resonators are intended for energy harvesting purpose and are designed to exhibit two-to-one internal resonance. In particular, we navigate the design space for the generalized V-shaped resonator to investigate the influence of shape parameters on the performance of the Vibration Energy Harvester. Notably, we introduce two metrics that help elucidating the role of the shape parameter in dictating the behavior of the system in terms of peak voltage and operational bandwidth width. For simplicity, we consider that the system is subjected to harmonic excitations near its primary resonances.

INTRODUCTION

The dynamical response of multi-member structures has been extensively studied over the past decades [1]. Perhaps, the simplest yet most studied multi-member structure is the L-shaped beam [2, 3, 4, 5, 6, 7, 8, 3, 9, 10, 11, 12, 13, 14, 15, 16], i.e. a structure that is composed of two members attached perpendicularly. Despite its simplicity, the L-shaped structure exhibits a rich dynamical behavior which includes: (a) energy exchange (pumping) between the modes of vibration [2, 3, 4, 5], (b) phase and amplitude modulations [6], (c) Hopf and saddle-node bifurcations [7, 8], (d) saturation phenomenon [3], and (e) chaotic vibrations [9]. Moreover, under certain geometric parameters, the L-shaped structure exhibits coupled torsional and out-of-plane bending modes [10, 11, 12, 13]. The internally resonant behavior of the L-shaped structure has been exploited, for instance, to widen the range of frequencies that energy can be extracted in vibrational energy harvesters [14, 15]. Additionally, the saturation phenomenon has been used to increase the average power scavenged when the harvester is subject to excitations that contain harmonic components and significant amounts of noise [16].

To design more efficient energy harvesters, Danzi *et. al* [17, 18, 19, 20, 21, 22] introduced the V-shaped resonator, i.e. a class

*Address all correspondence to this author.

of two-members structures that exhibit two-to-one internal resonance. Particularly, they noted that the space of feasible designs depends on the parameters defining the topology of the oscillator and is a manifold $S \in \mathbb{R}^{12}$ (see Figure 1). Moreover, they showed in [19] that solutions to the problem of having commensurate frequencies in a ratio two-to-one are quadratic functions of the members' length. Therefore, in most cases, two solutions are possible according to the members' lengths ratio. Using the same nomenclature adopted in [22], the two families of solutions, are dubbed the inner ($L_2/L_1 \leq 1$) and the outer ($L_2/L_1 > 1$) envelope respectively. Besides the length ratio L_2/L_1, and assuming that the Young's modulus and the density of the two members are equal, two other nondimensional parameters define the topology of the system, i.e the thickness ratio h_2/h_1 and the folding angle φ. In [22], they detailed how, leveraging topology, one can design a system whose nonlinear dynamical response exhibits: the co-existence of stable solutions, saddle-node bifurcations, modal interactions, and modal saturation. The above nonlinear dynamical behavior can be triggered at a frequency of interest by leveraging the effect of the folding angle; moreover, the resonators can be scaled by the Buckingham (π)-theorem to exhibit the same natural frequencies. Prompted by these results, here we extend the investigation of the dependency of shape parameters, performed in [22] for a mechanical system, to a Vibration Energy Harvester (VEH) device. In particular, we focus on the effect of the shape parameters on the voltage/energy that the system can harness and, the frequency bandwidth at which high amplitude vibrations can be sustained. We consider the case of harmonic excitations near the primary and secondary resonance of the system.

1 Consideration on the Mathematical Model

The mathematical model governing the finite amplitude vibrations for the generalized V-shaped resonator has been extensively discussed by Danzi *et al.* in [22]. In this manuscript, we de-emphasize the mathematical derivation in favor of a more in-depth understanding and interpretation of the results for the electro-mechanical model. Contrary to Danzi *et al.* [22], that considered only the mechanical model, we examine the coupled electro-mechnical system. In particular, we speculated that the piezo-electric transduction mechanism is (a) attached to the first member for a limited length thereafter indicated as L_p, (b) unimorph and, (c) its bending stiffness is negligible compared to that of the hosting structure. Following Harne *et al.* [16], we assumed that the transduction element has weak coupling effects of the mechanical equations of motion and hence the voltage of the device is proportional to the strain rate of the beam. The latter assumption allows us to write the expression of the voltage as

$$V_p(t) = -\theta \int_0^{L_p} \frac{\partial w_1^3(s_1,t)}{\partial^2 s_1 \partial t} \mathrm{d}s_1 \tag{1}$$

where θ is a coefficient related to the capacitance of the piezoelectric materials, the resistive load, the electro-mechanical coupling coefficient, and the lowest order short-circuit natural frequency of the system. In the equation in 1, w_1 is the bending displacement of the first beam member and s_1 is the curvilinear abscissa in the local reference frame.

For the class of thin multi-member structures considered herein, the model's complexity and the nonlinear order considered vary depending on the level of excitation provided. Indeed, if the excitation exceeds a certain threshold level, which depends on the stiffness and inertial properties of the resonator, third- or higher-order nonlinearities must be included [10]. Moreover, when the excitation exceeds the threshold level, one should also consider that the in-plane bending motion will no longer be decoupled from the out-of-plane bending and torsion [11]. Therefore, the complete model should include also the out-of plane bending displacement and the torsion. Contrarily, the results shown in the sequel are only valid if the resonator undergoes planar motion. Following [22], we limit the base excitation to $\ddot{w}_b = 1g$. For the resonators considered in this study, the onset of nonlinear responses was experimentally and numerically observed at a g-level as low as $\ddot{w}_b = 0.1g$ [22]; however, the motion of the system remains planar up to large g-levels which exceed the one considered herein. This justifies the set of assumptions listed below:

1. the beam members composing the resonators are inextensible; therefore, the longitudinal displacement u_i of the i^{th} member can be expressesd as

$$u_i \approx \int_0^{s_i} -\frac{1}{2}\left(\frac{dw_i}{ds_i}\right)^2 ds_i. \tag{2}$$

2. the resonators are composed of two prismatic, homogeneous and isotropic beams having the shear center aligned with the principal axis of inertia. The effect of transverse shear is neglected. Moreover, the effect of gravity is not included in the model;
3. only second order nonlinearities are retained as in [3] and the literature thereafter. The effect of higher order nonlinearities is neglected;
4. the system is subjected to finite amplitude vibrations and the motion of the multi-members beam lies at any time in the xy plane. Therefore, the effect of out of plane bending and torsion is neglected as in [3] and the citing literature thereafter;
5. motivated by the results reported by Danzi *et al.* [22], only proportional viscous damping is considered. In particular it is assumed that the modal damping coefficients associated to the first and second modes are equal and independent of the angle of orientation of the members.

The equations of motion assume the following form:

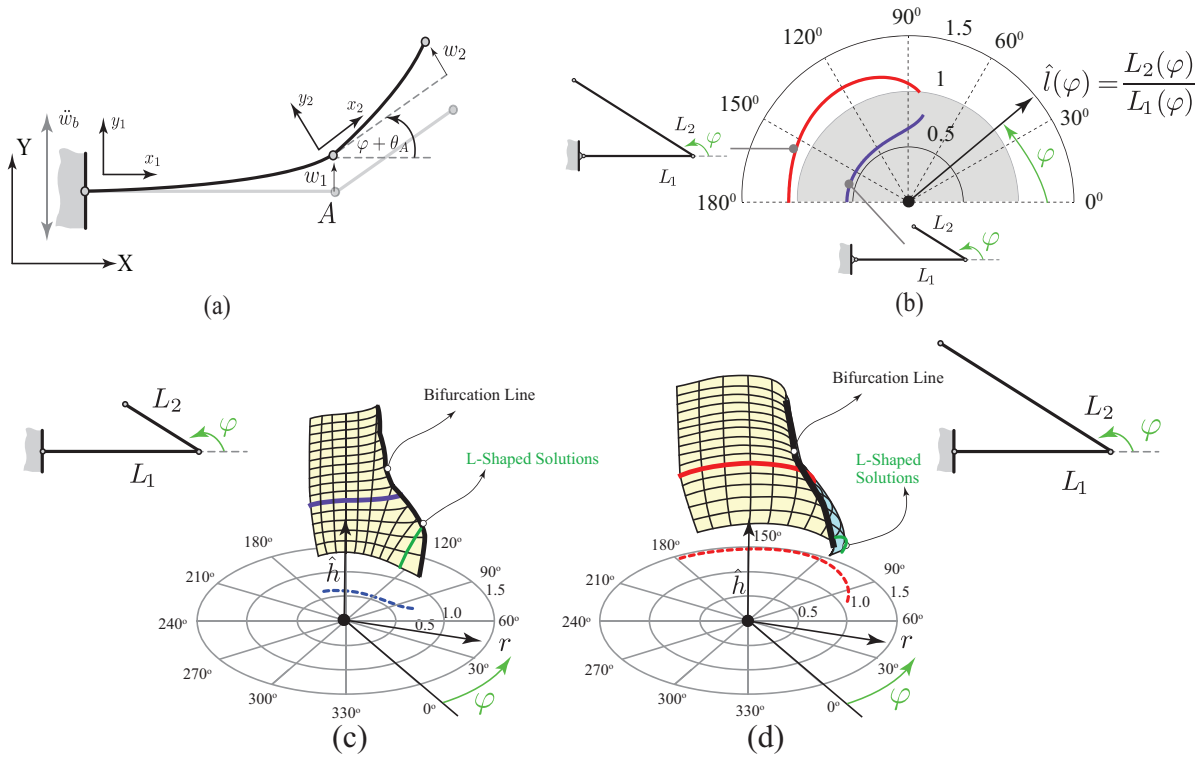

FIGURE 1: Generalized V-shaped resonator. (a) Exemplification of the deformed and undeformed structure. (b) Polar envelope at fixed thickness ratio ($\hat{h} = h_2/h_1 = 0.5$), (c,d) Polar representation of the 3D design envelope. The curves in red and blue correspond to the solutions depicted in (b) for the inner (c) and outer (d) envelope. The green curves in (c,d) represent the L-shaped solution.

$$\begin{bmatrix}1&0\\0&1\end{bmatrix}\begin{Bmatrix}\ddot{u}_1\\\ddot{u}_2\end{Bmatrix}+\begin{bmatrix}2\zeta_1&0\\0&2\zeta_2\eta\end{bmatrix}\begin{Bmatrix}\dot{u}_1\\\dot{u}_2\end{Bmatrix}+\begin{bmatrix}1&0\\0&\eta^2\end{bmatrix}\begin{Bmatrix}u_1\\u_2\end{Bmatrix}+\begin{bmatrix}\bar{a}_{11}&\bar{a}_{12}&\bar{a}_{13}\\\bar{a}_{21}&\bar{a}_{22}&\bar{a}_{23}\end{bmatrix}\begin{Bmatrix}\dot{u}_1^2\\\dot{u}_1\dot{u}_2\\\dot{u}_2^2\end{Bmatrix}+\begin{bmatrix}\bar{b}_{11}&\bar{b}_{12}&\bar{b}_{13}&\bar{b}_{14}\\\bar{b}_{21}&\bar{b}_{22}&\bar{b}_{23}&\bar{b}_{24}\end{bmatrix}\begin{Bmatrix}u_1\ddot{u}_1\\u_1\ddot{u}_2\\u_2\ddot{u}_1\\u_2\ddot{u}_2\end{Bmatrix}$$
$$+\ddot{w}_B\underbrace{\begin{bmatrix}\bar{c}_{11}&\bar{c}_{12}&\bar{c}_{13}\\\bar{c}_{21}&\bar{c}_{22}&\bar{c}_{23}\end{bmatrix}}_{f(\cos(\varphi))}\begin{Bmatrix}u_1^2\\u_1u_2\\u_2^2\end{Bmatrix}+\ddot{w}_B\underbrace{\begin{bmatrix}\bar{d}_{11}&\bar{d}_{12}\\\bar{d}_{21}&\bar{d}_{22}\end{bmatrix}}_{f(\sin(\varphi))}\begin{Bmatrix}u_1\\u_2\end{Bmatrix}+\dot{w}_B\underbrace{\begin{bmatrix}0&\bar{e}_{12}&0&\bar{e}_{14}\\\bar{e}_{21}&0&\bar{e}_{23}&0\end{bmatrix}}_{f(\cos(\varphi))}\begin{Bmatrix}u_1\dot{u}_1\\u_1\dot{u}_2\\u_2\dot{u}_1\\u_2\dot{u}_2\end{Bmatrix}=\ddot{w}_B\begin{Bmatrix}\bar{f}_1\\\bar{f}_2\end{Bmatrix},\tag{3}$$

where we introduced the nondimensional time $\tau = \omega t$ and displacement $\bar{w}_i = w_i/L_1$, and the transformation from physical to modal coordinates $\ddot{\mathbf{u}} = \mathbf{V}\ddot{\tilde{\mathbf{w}}}$, $\mathbf{V}$ are the mass normalized eigenvectors of the linear problem, $\mathbf{u}$ are the modal coordinates and, η is ratio of modal frequencies ω_2/ω_1. The lengthy expressions of the coefficients reported in the eqn. in 3 are omitted for brevity and can be found in [22]. The equation in 1 completes the system of equations governing the dynamics of the two members VEH.

Examining the electro-mechanical equation of motion reported in 3, it is worthwhile to notice that two of the parametric excitation terms reported therein are explicit functions of the cosine of the folding angle. These parametric excitations are zero for the case of the L-shaped beam while contribute to the rich dynamical behavior of the system when the angle differs from $\pi/2$. On the other hand, one could argue that the same applies when the folding angle is close to 0 or π; however, in this case,

solutions either do not exist $\varphi = 0$, or are unfeasible $\varphi = \pi$ because the two beam members overlap. In the following, we limit our investigation to the voltage amplitude and on the bandwidth width at which large amplitude of vibrations can be sustained. The next section introduces two metrics that are useful to compare the different VEHs' configurations.

2 Metrics Adopted for the Comparative Study

Restricting the vibration energy harvesters to be subject to a harmonic excitation, its performance can be characterized by two metrics, the peak power it harvests and its bandwidth [23]. These metrics arise naturally when considering that harmonic excitations can be grouped into (a) fixed frequency excitation, and (b) fixed frequency excitation that drifts. If the harmonic excitation has a fixed frequency then the peak power at that frequency must be maximized regardless of the harvester's bandwidth. If the harmonic excitation has a frequency that slightly drifts around a center value, then the peak power and the bandwidth around the central frequency are both important for optimal scavenging. Here, we will arbitrarily define bandwidth as the difference in the frequency where the occurrences of jump from the low amplitude response trajectory to the higher amplitude response trajectory and the subsequent downward jump is observed. Alternatively, one could adopt the definition given in [24], where the low amplitude solution branches were considered to define the SDOF vibration energy harvester in presence of co-existing low-amplitude and high-amplitude branches. The peak power will be defined as the high amplitude response at the jump. An exemplification of two metrics adopted in this analysis is depicted in Figure 2.

3 Approximate Solution to Governing Equations

We seek approximate solutions to the nonlinear equations governing the dynamics of the systems through the method of multiple time scales. We defined the n^{th} time scale as $T_n = \varepsilon^n t$ where ε is a small bookkeeping parameter, furthermore the constants are scaled to ε. This allows the time derivatives to be written as

$$\frac{d}{dt} = D_0 + \varepsilon D_1 + \mathcal{O}(\varepsilon^2), \tag{4a}$$

$$\frac{d^2}{dt^2} = D_0^2 + 2\varepsilon D_0 D_1 + \mathcal{O}(\varepsilon^2), \tag{4b}$$

where $D_n = \partial/\partial T_n$. Additionally, we expand u_1 and u_2 as

$$u_1(t) = u_{10}(T_0, T_1) + \varepsilon u_{11}(T_0, T_1) + \mathcal{O}(\varepsilon^2), \tag{5a}$$

$$u_2(t) = u_{20}(T_0, T_1) + \varepsilon u_{21}(T_0, T_1) + \mathcal{O}(\varepsilon^2). \tag{5b}$$

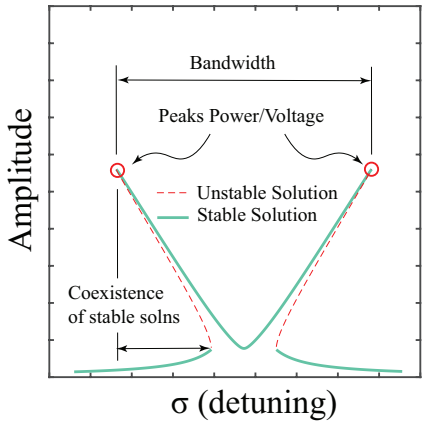

FIGURE 2: Exemplification of the nonlinear response (Amplitude vs frequency) of the V-shaped resonator. The figure shows the general frequency response function with bifurcation and co-existence of stable solutions. The two metrics adopted in this manuscript are annotated in the figure to emphasize their physical significance.

Finally, the constant parameters are scaled such that the coefficients of the nonlinear terms, forcing and damping are scaled to the order epsilon

$\mathcal{O}(\varepsilon^0)$:

$$D_0^2 u_{10} + u_{10} = 0, \tag{6a}$$

$$D_0^2 u_{20} + \eta^2 u_{20} = 0, \tag{6b}$$

$\mathcal{O}(\varepsilon^1)$:

$$\begin{aligned} D_0^2 u_{11} + u_{11} = &-2D_0 D_1 u_{10} - 2\zeta_1 D_0 u_{10} \\ &- \bar{a}_{11}(D_0 u_{10})^2 - \bar{a}_{12} D_0 u_{10} D_0 u_{20} - \bar{a}_{13}(D_0 u_{20})^2 \\ &- \bar{b}_{11}(D_0^2 u_{10}) u_{10} - \bar{b}_{12}(D_0^2 u_{20}) u_{10} \\ &- \bar{b}_{13}(D_0^2 u_{10}) D_0 u_{20} - \bar{b}_{14}(D_0^2 u_{20}) u_{20} \quad + g\bar{f}_1 \cos\bar{\Omega} t, \end{aligned} \tag{7a}$$

$$\begin{aligned} D_0^2 u_{21} + \eta^2 u_{21} = &-2D_0 D_1 u_{20} - 2\zeta_2 \eta D_0 u_{20} \\ &- \bar{a}_{21}(D_0 u_{10})^2 - \bar{a}_{22} D_0 u_{10} D_0 u_{20} - \bar{a}_{23}(D_0 u_{20})^2 \\ &- \bar{b}_{21}(D_0^2 u_{10}) u_{10} - \bar{b}_{22}(D_0^2 u_{20}) u_{10} - \bar{b}_{23}(D_0^2 u_{10}) D_0 u_{20} \\ &- \bar{b}_{24}(D_0^2 u_{20}) u_{20} + g\bar{f}_2 \cos\bar{\Omega} t. \end{aligned} \tag{7b}$$

The solution to order epsilon to the order zero-th problem can be written as

$$u_{10} = A_1(T_1)e^{iT_0} + cc, \quad \text{and} \quad u_{20} = A_2(T_1)e^{i\eta T_0} + cc. \tag{8}$$

Which allows the order $\mathscr{O}(\varepsilon^1)$ problem to be written as

$$\begin{aligned} D_0^2 u_{11} + u_{11} = &-2i(D_1+\zeta_1)A_1 e^{iT_0} + (\bar{a}_{11}+\bar{b}_{11})A_1^2 e^{2iT_0} \\ &+ (\bar{a}_{12}\eta + \bar{b}_{12}\eta^2 + \bar{b}_{13})A_1 A_2 e^{i(\eta+1)T_0} \\ &+ (\bar{a}_{13}+\bar{b}_{14})\eta^2 A_2^2 e^{2i\eta T_0} \\ &+ (\bar{b}_{13} - \bar{a}_{12} + \bar{b}_{12}\eta^2)\bar{A}_1 A_2 e^{i(\eta-1)T_0} \\ &- (\bar{a}_{11}+\bar{b}_{11})A_1\bar{A}_1 \\ &- (\bar{a}_{13}+\bar{b}_{14})\eta^2 A_2\bar{A}_2 + \frac{1}{2}g\bar{f}_1 e^{i\Omega T_0} + cc, \end{aligned} \tag{9a}$$

$$\begin{aligned} D_0^2 u_{21} + \eta^2 u_{21} = &-2i(D_2+\zeta_2)A_2 e^{iT_0} + (\bar{a}_{21}+\bar{b}_{12})A_1^2 e^{2iT_0} \\ &+ (\bar{a}_{22}\eta + \bar{b}_{22}\eta^2 + \bar{b}_{23})A_1 A_2 e^{i(\eta+1)T_0} \\ &+ (\bar{a}_{23}+\bar{b}_{24})\eta^2 A_2^2 e^{2i\eta T_0} \\ &+ (\bar{b}_{23} - \bar{a}_{12} + \bar{b}_{12}\eta^2)\bar{A}_1 A_2 e^{i(\eta-1)T_0} \\ &- (\bar{a}_{21}+\bar{b}_{21})A_1\bar{A}_1 \\ &- (\bar{a}_{23}+\bar{b}_{24})\eta^2 A_2\bar{A}_2 + \frac{1}{2}g\bar{f}_2 e^{i\Omega T_0} + cc. \end{aligned} \tag{9b}$$

In the following, using the two metrics detailed above, we analyze the performance of the system when it is excited with a frequency near the primary frequencies. While the mechanical model is solved using the method of multiple scales, the voltage equation is solved numerically by means of the Dormand-Prince method (Matlab *ode45*).

3.1 Excitation near the primary resonance: $\Omega \approx 1$

In the first case, we introduce the following transformation

$$\Omega = 1 + \varepsilon\sigma_0, \quad \eta = 2 + \varepsilon\sigma_1, \tag{10a}$$

$$\text{with } \Omega \approx 1 \quad \text{and} \quad \eta \approx 2. \tag{10b}$$

where σ_0 and σ_1 are the detuning parameters between the first modal frequency and, respectively, the excitation frequency and the second modal frequency. Substituting the above equations, eliminating secular terms in the fast time scale T_0, introducing the polar transformation $A_1 = a_1 \exp i\beta_1$ and $A_2 = a_2 \exp i\beta_2$ and separating real and imaginary parts, the following slow amplitude equations are found

$$\begin{aligned} a_1\beta_1' + a_1 a_2 \frac{\Gamma_1}{4}\cos(\gamma_1) + \frac{1}{2}f_1 g\cos(\gamma_0) = 0, \\ a_1' + \zeta_1 a_1 - a_1 a_2 \frac{\Gamma_1}{4}\sin(\gamma_1) - \frac{1}{2}f_1 g\sin(\gamma_0) = 0, \end{aligned} \tag{11}$$

and

$$\begin{aligned} \eta a_2\beta_2' + \frac{\Gamma_2}{4}\cos(\gamma_1) = 0, \\ \eta a_2' + \eta^2 a_2 - \frac{\Gamma_2}{4}a_1^2\sin(\gamma_1) = 0, \end{aligned} \tag{12}$$

where a_i are the amplitudes while β_i are the phases and where the prime ($'$) represents derivative w.r.t the nondimensional time. For a detailed explanation of the coefficients, the reader is addressed to [22].

3.2 Excitation near the secondary resonance: $\Omega \approx \eta$

Likewise, to investigate the performance of the resonator when the system is excited near the secondary modal frequency ($\Omega \approx \eta$) and when the second modal frequency is nearly twice the first modal frequency ($\eta \approx 2$), we introduce the following

$$\eta = 2 + \varepsilon\sigma_1 \quad \Omega = 2 + \varepsilon\sigma_2, \tag{13}$$

here σ_1 and σ_2 are the parameters describing the detuning between the first and second modal frequency, the second modal frequency and, respectively, the excitation frequency. This yields the following amplitude equation

$$-2i(D_1+\zeta_1)A_1 + \Gamma_1\bar{A}_1 A_2 e^{i\sigma_1 T_1} = 0, \tag{14}$$

$$-2i(\eta D_1 + \eta^2\zeta_2)A_2 + \Gamma_2 A_1^2 e^{-i\sigma_1 T_1} + \frac{1}{2}g f_2 e^{i\sigma_2 T_1} = 0, \tag{15}$$

Again, applying the polar transformation and separating real and imaginary parts yields the following

$$a_1' + \zeta_1 a_1 - \frac{\Gamma_1}{4}a_1 a_2 \sin\gamma_1 = 0, \tag{16a}$$

$$\beta_1' a_1 + \frac{\Gamma_1}{4}a_1 a_2 \cos\gamma_1 = 0, \tag{16b}$$

$$\eta\beta_2' a_2 + \frac{\Gamma_2}{4}a_1^2\cos\gamma_1 + \frac{1}{2}f_2 g\cos\gamma_2 = 0, \tag{16c}$$

$$\eta a_2' + \eta^2 a_2 + \frac{\Gamma_2}{4}a_1^2\sin\gamma_1 - \frac{1}{2}f_2 g\sin\gamma_2 = 0. \tag{16d}$$

where the constants γ_1 and γ_2 can be expressed as

$$\gamma_1 = \sigma_1 T_1 - 2\beta_1 + \beta_2, \quad \text{and} \quad \gamma_2 = \sigma_2 T_2 - \beta_2. \tag{17}$$

the low amplitude solution [3] that excited the second vibration mode can be written as

$$\begin{aligned} a_1 =& 0, \quad \gamma_1 = \text{indeterminate, and} \\ a_2 =& \frac{g f_2}{2\eta\sqrt{\sigma_2^2 + \eta^2\zeta_2^2}}, \quad \text{and} \quad \tan\gamma_2 = \frac{-\eta\zeta_2}{\sigma_2}, \end{aligned} \tag{18}$$

The second solution can be instead written as

$$\begin{aligned} a_1^2 =& \frac{8\eta(\sigma_2(\sigma_1+\sigma_2) - 2\eta\zeta_1\zeta_2)}{\Gamma_1^2\Gamma_2^2} \\ & \pm 2\sqrt{g^2\Gamma_1^2 f_2^2 - 16\eta^2(2\sigma_2\zeta_1 + \eta(\sigma_1+\sigma_2)\zeta_2)^2}, \end{aligned} \tag{19a}$$

$$a_2 = \frac{2\sqrt{(\sigma_1+\sigma_2)^2 + 4\zeta_1^2}}{\Gamma_1}, \tag{19b}$$

$$\tan\gamma_1 = \frac{-2\zeta_1}{\sigma_1+\sigma_2}, \quad \text{and} \tag{19c}$$

$$\tan\gamma_2 = \frac{2\Gamma_2 a_1^2 + \Gamma_1\eta^2 a_2\zeta_2}{\Gamma_2(\sigma_1+\sigma_2)a_1^2 - 2\Gamma_1\eta\sigma_2 a_2^2}. \tag{19d}$$

The stability of each equilibrium solution is determined by finding the eigenvalues of the Jacobian matrix of the modulation equations and is not discussed here.

4 Results and Discussion

In analyzing the V-shaped resonator, the excitation will have sufficient energy to activate the nonlinear response of the VEH. Based on our prior investigation of the mechanical model [22], base excitations as low as $\ddot{w}_b = 0.1g$ are sufficient to trigger the nonlinear response. We speculated that the effect of the piezoelectric patch has a negligible effect on the elastic response of the system. For simplicity, the excitation level will be held constant and equal to $\ddot{w}_b = 1g$ independently of the configuration of the resonator considered.

In the following, we will compare the response of three classes of resonators, respectively $\hat{h} = 0.5$, $\hat{h} = 1$, and $\hat{h} = 2$ at various angle of orientations. At any given nondimensional thickness $\hat{h}$, we will compare solutions with the following discrete set of folding angle $\varphi = 80, 90, 120, 135, 160$ degrees, provided that solutions exist. Indeed, as noted in [19], when the nondimensional thickness $\hat{h}$ increases, the domain of existence of solutions that exhibit commensurate frequencies in a ratio two-to-one is limited to a narrow region in the second quadrant ($\pi/2 < \varphi < \pi$). For simplicity we will use the same compact notation adopted in [22], i.e. ${}^{\hat{h}}V^{O}$ where O indicated that the solutions considered are those of the outer envelope $\hat{l} > 1$. As already shown by Danzi *et al.* [22], those solutions are advantageous in terms of bandwidth at which high amplitude vibrations are sustained. This is mainly due to the fact that the second beam is longer than the first member and therefore the system is more flexible.

We consider that all the resonators are made of Aluminum ($E = 68.9$ GPa, and $\nu = 0.3$); moreover, we assume that all the beam members have the same width $b = 12$ mm. The piezoelectric patch has the following dimensional parameters: length $L_P = 50$ mm, piezoelectric strain constant $d_{31} = 30$ pC/N, relative dielectric constant $\varepsilon_{33}/\varepsilon_0 = 12$, density $\rho = 1700$ kg/m^3, thickness $t_p = 0.5$ mm. For simplicity, we assume that the resistance is equal for all the resonators and in particular $R = 15.6$ MΩ.

Analyzing the results reported in Figure 3, the following trends are noteworthy;

1. larger level of vibrations and peak Voltage can be attained when the system is excited near the second resonance ($\eta = 2$). We speculate that this is due to the modal energy exchange (energy pumping) discussed in [3] and observed also for the V-shaped resonator in [22];
2. when the excitation is near the second resonance, the bandwidth at which large amplitude vibration are sustained is larger w.r.t. the case in which the system is excited near the first resonance.
3. when the system is excited near the second resonance, the maximum bandwidth corresponds to solutions whose folding angle is in the region between 120 and 140 degrees;
4. to maximize the peak voltage, it is advantageous to consider solution as close as possible to the lower bound of the possible folding angle.

5 Conclusions

This manuscript considers the nonlinear behavior of a V shaped vibration-based energy harvester. The harvester has commensurate frequencies yielding an internally resonant structure. The modal behavior of the resonator was determined using a nonlinear reduced order model. The nonlinear equations of motion were solved employing the method of multiple time scales for the mechanical part while, the solutions to the voltage equation were calculated using a Runge-kutta method (Matlab ode45). While only discrete values of the folding angles were considered, it was found that a combination of excitation frequency, length ratio and folding angle affected both the peak power and bandwidth of the harvester.

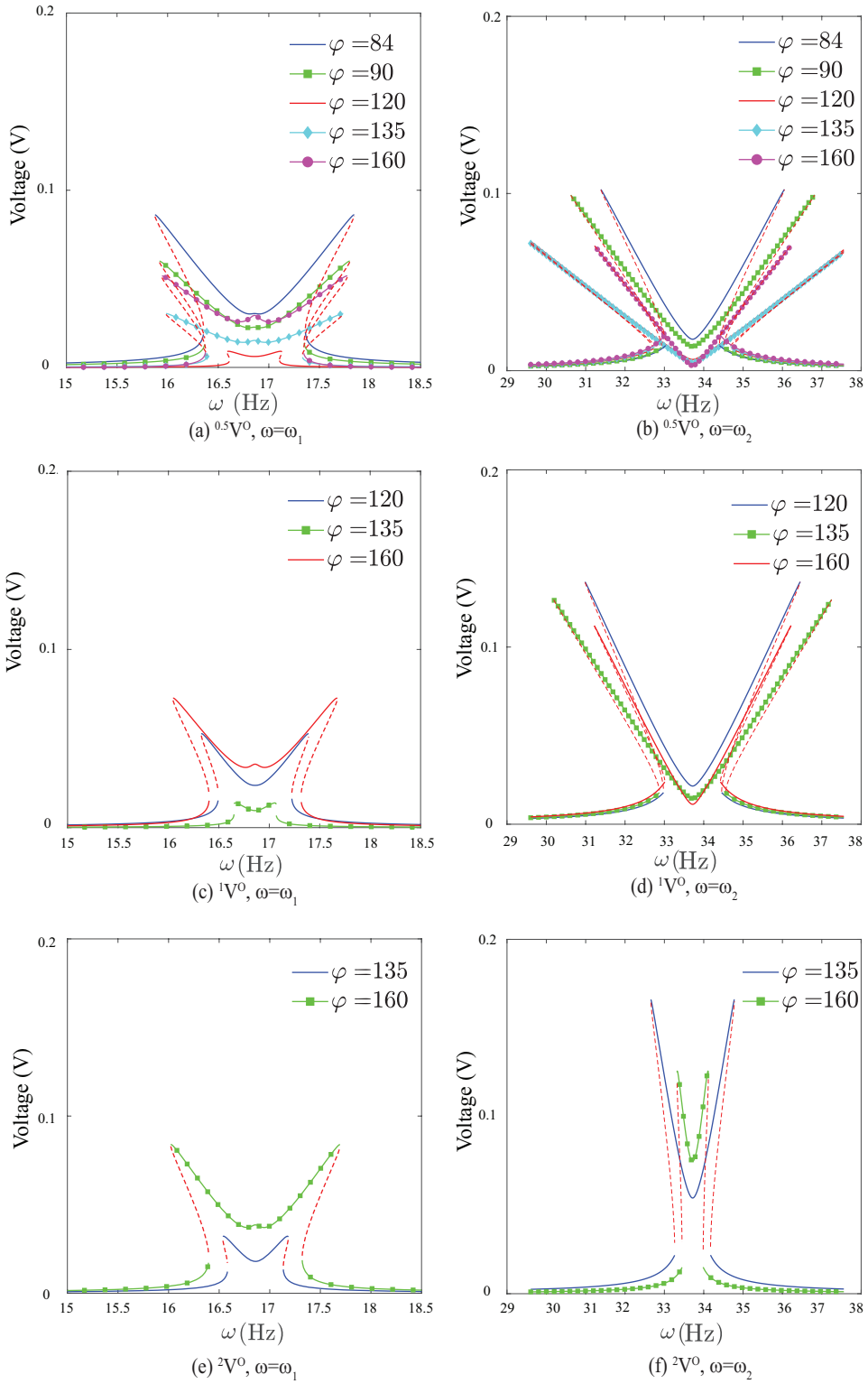

FIGURE 3: Voltage frequency responses for various resonators of the outer envelope under 1g base excitation. The system is excited at the first (a,c,e) and second resonance (b,d,f) respectively.

ACKNOWLEDGMENT

The authors would like to acknowledge the financial support provided by NSF CAREER Award: CMMI 2145803 and the Purdue Research Foundation (PRF).

REFERENCES

[1] Hurty, W. C. "Vibrations of structural systems by component mode synthesis." *Journal of the Engineering Mechanics Division* Vol. 86 (1960): pp. 51–70.

[2] Cartmell, MP and Roberts, JW. "Simultaneous combination resonances in a parametrically excited cantilever beam." *Strain* Vol. 23 No. 3 (1987): pp. 117–126.

[3] Haddow, AG, Barr, ADS and Mook, DT. "Theoretical and experimental study of modal interaction in a two-degree-of-freedom structure." *Journal of Sound and Vibration* Vol. 97 No. 3 (1984): pp. 451–473.

[4] Roberts, JW and Cartmell, MP. "Forced vibration of a beam system with autoparametric coupling effects." *Strain* Vol. 20 No. 3 (1984): pp. 123–131. doi:10.1111/j.1475-1305.1984.tb00542.x.

[5] Nayfeh, A. H., Balachandran, B., Colbert, M. A. and Nayfeh, M. A. "An experimental investigation of complicated responses of a two-degree-of-freedom structure." *Journal of Applied Mechanics* Vol. 56 No. 4 (1989): pp. 960–967. doi:10.1115/1.3176197. URL https://doi.org/10.1115/1.3176197.

[6] Nayfeh, A.H. and Zavodney, L.D. "The response of two-degree-of-freedom systems with quadratic non-linearities to a combination parametric resonance." *Journal of Sound and Vibration* Vol. 107 No. 2 (1986): pp. 329 – 350. doi:https://doi.org/10.1016/0022-460X(86)90242-7. URL http://www.sciencedirect.com/science/article/pii/0022460X86902427.

[7] Arafat, Haider N., Nayfeh, Ali H. and Chin, Char-Ming. "Nonlinear nonplanar dynamics of parametrically excited cantilever beams." *Nonlinear Dynamics* Vol. 15 No. 1 (1998): pp. 31–61. doi:10.1023/A:1008218009139. URL https://doi.org/10.1023/A:1008218009139.

[8] Balachandran, B and Nayfeh, AH. "Nonlinear motions of beam-mass structure." *Nonlinear Dynamics* Vol. 1 No. 1 (1990): pp. 39–61.

[9] Yu, Tian-Jun, Zhang, Wei and Yang, Xiao-Dong. "Global bifurcations and chaotic motions of a flexible multi-beam structure." *International Journal of Non-Linear Mechanics* Vol. 95 (2017): pp. 264 – 271. doi:https://doi.org/10.1016/j.ijnonlinmec.2017.06.015. URL http://www.sciencedirect.com/science/article/pii/S0020746217300239.

[10] Warminski, J, Cartmell, M.P, Bochenski, M and Ivanov, Ivelin. "Analytical and experimental investigations of an autoparametric beam structure." *Journal of Sound and Vibration* Vol. 315 No. 3 (2008): pp. 486–508.

[11] Georgiades, Fotios. "Nonlinear equations of motion of L-shaped beam structures." *European Journal of Mechanics - A/Solids* Vol. 65 (2017): pp. 91 – 122. doi:https://doi.org/10.1016/j.euromechsol.2017.03.007. URL http://www.sciencedirect.com/science/article/pii/S0997753816301218.

[12] Bux, S.L. and Roberts, J.W. "Non-linear vibratory interactions in systems of coupled beams." *Journal of Sound and Vibration* Vol. 104 No. 3 (1986): pp. 497 – 520. doi:https://doi.org/10.1016/0022-460X(86)90304-4. URL http://www.sciencedirect.com/science/article/pii/0022460X86903044.

[13] Nayfeh, A.H. and Balachandran, B. "Experimental investigation of resonantly forced oscillations of a two-degree-of-freedom structure." *International Journal of Non-Linear Mechanics* Vol. 25 No. 2 (1990): pp. 199 – 209. doi:10.1016/0020-7462(90)90051-A. URL https://doi.org/10.1016/0020-7462(90)90051-A.

[14] Cao, DX, Leadenham, S and Erturk, A. "Internal resonance for nonlinear vibration energy harvesting." *The European Physical Journal Special Topics* Vol. 224 No. 14-15 (2015): pp. 2867–2880.

[15] Chen, Li-Qun, Jiang, Wen-An, Panyam, Meghashyam and Daqaq, Mohammed F. "A broadband internally resonant vibratory energy harvester." *Journal of Vibration and Acoustics* Vol. 138 No. 6 (2016): p. 061007.

[16] Harne, RL, Sun, A and Wang, KW. "Leveraging nonlinear saturation-based phenomena in an L-shaped vibration energy harvesting system." *Journal of Sound and Vibration* Vol. 363 (2016): pp. 517–531.

[17] Danzi, Francesco, Gibert, James M., Cestino, Enrico and Frulla, Giacomo. "Topology synthesis of planar ground structures for energy harvesting applications." Park, Gyuhae (ed.). *Active and Passive Smart Structures and Integrated Systems 2017*, Vol. 10164: pp. 365 – 382. 2017. International Society for Optics and Photonics, SPIE. doi:10.1117/12.2257351. URL https://doi.org/10.1117/12.2257351.

[18] Danzi, Francesco, Gibert, James M., Frulla, Giacomo and Cestino, Enrico. "Graph-based element removal method for topology synthesis of beam based ground structures." *Structural and Multidisciplinary Optimization* doi:10.1007/s00158-017-1818-x. URL https://doi.org/10.1007/s00158-017-1818-x.

[19] Danzi, Francesco, Gibert, James M., Frulla, Giacomo and Cestino, Enrico. "Generalized topology for resonators having N commensurate harmonics." *Journal of Sound and Vibration* Vol. 419 (2018): pp. 585 – 603. doi:10.1016/j.jsv.2017.10.001.

[20] Danzi, F. "Dynamic tailoring of beam-like

structures. Application to high aspect ratio unitized box-beam and internal resonant structures." Ph.D. Thesis, Politecnico di Torino. 2018. doi:https://doi.org/10.6092/polito/porto/2712259.

[21] Danzi, Francesco and Gibert, James M. "Exact dynamics of an angle-shaped resonator for energy scavenging applications." Erturk, Alper (ed.). *Active and Passive Smart Structures and Integrated Systems XII*, Vol. 10595: pp. 669 – 686. 2018. International Society for Optics and Photonics, SPIE. doi:10.1117/12.2296642. URL https://doi.org/10.1117/12.2296642.

[22] Danzi, Francesco, Tao, Hongcheng and Gibert, James M. "The role of topology on the response of a V-shaped resonator." *Nonlinear Dynamics* Vol. 101 No. 4 (2020): pp. 2027–2053. doi:10.1007/s11071-020-05789-y.

[23] *New Insights Into Piezoelectric Energy Harvesting Using a Dynamic Magnifier*, Vol. Volume 2: Mechanics and Behavior of Active Materials; Integrated System Design and Implementation; Bio-Inspired Materials and Systems; Energy Harvesting of *Smart Materials, Adaptive Structures and Intelligent Systems* (2012). doi:10.1115/SMASIS2012-8086.

[24] Quinn, D. Dane, Triplett, Angela L., Bergman, Lawrence A. and Vakakis, Alexander F. "Comparing Linear and Essentially Nonlinear Vibration-Based Energy Harvesting." *Journal of Vibration and Acoustics* Vol. 133 No. 1. doi:10.1115/1.4002782.